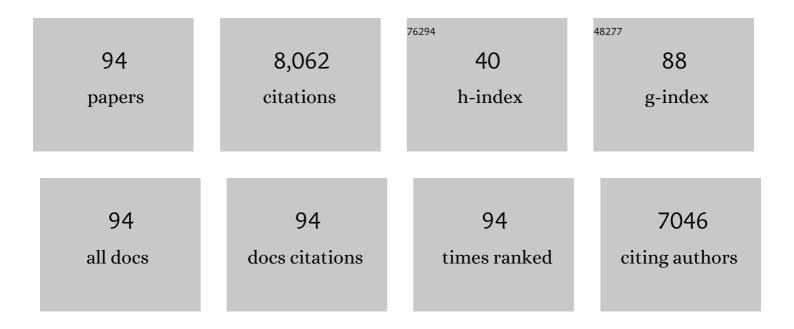
List of Publications by Year in descending order

Source: https://exaly.com/author-pdf/6370429/publications.pdf Version: 2024-02-01



#	Article	IF	CITATIONS
1	Microstructure evolution and critical stress for twinning in the CrMnFeCoNi high-entropy alloy. Acta Materialia, 2016, 118, 152-163.	3.8	823
2	Reasons for the superior mechanical properties of medium-entropy CrCoNi compared to high-entropy CrMnFeCoNi. Acta Materialia, 2017, 128, 292-303.	3.8	803
3	Design of a twinning-induced plasticity high entropy alloy. Acta Materialia, 2015, 94, 124-133.	3.8	618
4	Degradation Mechanisms of Pt/C Fuel Cell Catalysts under Simulated Start–Stop Conditions. ACS Catalysis, 2012, 2, 832-843.	5.5	470
5	On the formation and growth of intermetallic phases during interdiffusion between low-carbon steel and aluminum alloys. Acta Materialia, 2011, 59, 1586-1600.	3.8	397
6	On the contribution of carbides and micrograin boundaries to the creep strength of tempered martensite ferritic steels. Acta Materialia, 2007, 55, 539-550.	3.8	234
7	Stability investigations of electrocatalysts on the nanoscale. Energy and Environmental Science, 2012, 5, 9319.	15.6	230
8	Smaller is less stable: Size effects on twinning vs. transformation of reverted austenite in TRIP-maraging steels. Acta Materialia, 2014, 79, 268-281.	3.8	225
9	Segregation Stabilizes Nanocrystalline Bulk Steel with Near Theoretical Strength. Physical Review Letters, 2014, 113, 106104.	2.9	224
10	Hierarchical microstructure of explosive joints: Example of titanium to steel cladding. Materials Science & Engineering A: Structural Materials: Properties, Microstructure and Processing, 2011, 528, 2641-2647.	2.6	214
11	Microstructural evolution of a Ni-based superalloy (617B) at 700°C studied by electron microscopy and atom probe tomography. Acta Materialia, 2012, 60, 1731-1740.	3.8	212
12	Influence of intermetallic phases and Kirkendall-porosity on the mechanical properties of joints between steel and aluminium alloys. Materials Science & Engineering A: Structural Materials: Properties, Microstructure and Processing, 2011, 528, 4630-4642.	2.6	209
13	Phase stability and kinetics of Ï <i>f</i> -phase precipitation in CrMnFeCoNi high-entropy alloys. Acta Materialia, 2018, 161, 338-351.	3.8	209
14	Metallic composites processed via extreme deformation: Toward the limits of strength in bulk materials. MRS Bulletin, 2010, 35, 982-991.	1.7	180
15	Friction-stir dissimilar welding of aluminium alloy to high strength steels: Mechanical properties and their relation to microstructure. Materials Science & Engineering A: Structural Materials: Properties, Microstructure and Processing, 2012, 556, 175-183.	2.6	161
16	The nucleation of Mo-rich Laves phase particles adjacent to M23C6 micrograin boundary carbides in 12% Cr tempered martensite ferritic steels. Acta Materialia, 2015, 90, 94-104.	3.8	140
17	On the nucleation of Laves phase particles during high-temperature exposure and creep of tempered martensite ferritic steels. Acta Materialia, 2014, 81, 230-240.	3.8	129
18	Advanced Scale Bridging Microstructure Analysis of Single Crystal Niâ€Base Superalloys. Advanced Engineering Materials, 2015, 17, 216-230.	1.6	117

#	Article	IF	CITATIONS
19	Stability of Dealloyed Porous Pt/Ni Nanoparticles. ACS Catalysis, 2015, 5, 5000-5007.	5.5	110
20	Interaction of Cobalt Nanoparticles with Oxygen- and Nitrogen-Functionalized Carbon Nanotubes and Impact on Nitrobenzene Hydrogenation Catalysis. ACS Catalysis, 2014, 4, 1478-1486.	5.5	108
21	Microstructure and mechanical properties of magnesium alloy AZ31B laser beam welds. Materials Science & Engineering A: Structural Materials: Properties, Microstructure and Processing, 2008, 485, 20-30.	2.6	98
22	The structural and electronic promoting effect of nitrogen-doped carbon nanotubes on supported Pd nanoparticles for selective olefin hydrogenation. Catalysis Science and Technology, 2013, 3, 1964.	2.1	79
23	Double minimum creep of single crystal Ni-base superalloys. Acta Materialia, 2016, 112, 242-260.	3.8	74
24	Nanoindentation studies of the mechanical properties of the μ phase in a creep deformed Re containing nickel-based superalloy. Materials Science & Engineering A: Structural Materials: Properties, Microstructure and Processing, 2015, 634, 202-208.	2.6	72
25	Accelerated atomic-scale exploration of phase evolution in compositionally complex materials. Materials Horizons, 2018, 5, 86-92.	6.4	72
26	Columnar to equiaxed transition and grain refinement of cast CrCoNi medium-entropy alloy by microalloying with titanium and carbon. Journal of Alloys and Compounds, 2019, 775, 1068-1076.	2.8	71
27	Microstructure refinement for high modulus in-situ metal matrix composite steels via controlled solidification of the system Fe–TiB2. Acta Materialia, 2015, 96, 47-56.	3.8	68
28	Microstructure and Mechanical Properties of an AA6181â€₹4 Aluminium Alloy to HC340LA High Strength Steel Friction Stir Overlap Weld. Advanced Engineering Materials, 2008, 10, 961-972.	1.6	66
29	Understanding precipitate evolution during friction stir welding of Al-Zn-Mg-Cu alloy through in-situ measurement coupled with simulation. Acta Materialia, 2018, 148, 163-172.	3.8	64
30	Crystallization, phase evolution and corrosion of Fe-based metallic glasses: An atomic-scale structural and chemical characterization study. Acta Materialia, 2014, 71, 20-30.	3.8	62
31	Tempering behavior of a low nitrogen boron-added 9%Cr steel. Materials Science & Engineering A: Structural Materials: Properties, Microstructure and Processing, 2016, 662, 443-455.	2.6	62
32	Deformationâ€Induced Martensite: A New Paradigm for Exceptional Steels. Advanced Materials, 2016, 28, 7753-7757.	11.1	61
33	Influence of composition and precipitation evolution on damage at grain boundaries in a crept polycrystalline Ni-based superalloy. Acta Materialia, 2019, 166, 158-167.	3.8	61
34	Mechanisms of subgrain coarsening and its effect on the mechanical properties of carbon-supersaturated nanocrystalline hypereutectoid steel. Acta Materialia, 2015, 84, 110-123.	3.8	60
35	Microstructure and mechanical properties of Al0.7CoCrFeNi high-entropy-alloy prepared by directional solidification. Intermetallics, 2018, 93, 93-100.	1.8	60
36	Ledges and grooves at γ/γ′ interfaces of single crystal superalloys. Acta Materialia, 2015, 90, 105-117.	3.8	49

#	Article	IF	CITATIONS
37	Kinetics and crystallization path of a Fe-based metallic glass alloy. Acta Materialia, 2017, 127, 341-350.	3.8	47
38	EBSD Technique Visualization of Material Flow in Aluminum to Steel Frictionâ€stir Dissimilar Welding. Advanced Engineering Materials, 2008, 10, 1127-1133.	1.6	45
39	Influence of micro-blasting on the microstructure and residual stresses of CVD κ-Al2O3 coatings. Surface and Coatings Technology, 2009, 203, 3708-3717.	2.2	43
40	Effect of Shot-peening on the Oxidation Behaviour of Boiler Steels. Oxidation of Metals, 2011, 76, 233-245.	1.0	41
41	Control of Phase Coexistence in Calcium Tantalate Composite Photocatalysts for Highly Efficient Hydrogen Production. Chemistry of Materials, 2013, 25, 4739-4745.	3.2	41
42	On Local Phase Equilibria and the Appearance of Nanoparticles in the Microstructure of Singleâ€Crystal Niâ€Base Superalloys. Advanced Engineering Materials, 2016, 18, 1556-1567.	1.6	39
43	On the nucleation of planar faults during low temperature and high stress creep of single crystal Ni-base superalloys. Acta Materialia, 2018, 144, 642-655.	3.8	39
44	Atomic-scale investigation of fast oxidation kinetics of nanocrystalline CrMnFeCoNi thin films. Journal of Alloys and Compounds, 2018, 766, 1080-1085.	2.8	39
45	Stress-induced formation of TCP phases during high temperature low cycle fatigue loading of the single-crystal Ni-base superalloy ERBO/1. Acta Materialia, 2019, 168, 343-352.	3.8	39
46	Microstructure evolution in refill friction stir spot weld of a dissimilar Al–Mg alloy to Zn-coated steel. Science and Technology of Welding and Joining, 2017, 22, 658-665.	1.5	37
47	Influence of nitridation on surface microstructure and properties of graded cemented carbides with Co and Ni binders. Surface and Coatings Technology, 2008, 202, 5962-5975.	2.2	36
48	Simple synthesis of superparamagnetic magnetite nanoparticles as highly efficient contrast agent. Materials Letters, 2013, 95, 186-189.	1.3	35
49	The crystallographic template effect assisting the formation of stable α-Al2O3 during low temperature oxidation of Fe–Al alloys. Corrosion Science, 2016, 105, 100-108.	3.0	34
50	How evolving multiaxial stress states affect the kinetics of rafting during creep of single crystal Ni-base superalloys. Acta Materialia, 2018, 158, 381-392.	3.8	32
51	Long-term microstructural stability of oxide-dispersion strengthened Eurofer steel annealed at 800A°C. Journal of Nuclear Materials, 2014, 448, 33-42.	1.3	30
52	Design and Characterization of Novel Wear Resistant Multilayer CVD Coatings with Improved Adhesion Between Al ₂ O ₃ and Ti(C,N). Advanced Engineering Materials, 2010, 12, 929-934.	1.6	29
53	Thermal stability of TiAlN/CrN multilayer coatings studied by atom probe tomography. Ultramicroscopy, 2011, 111, 518-523.	0.8	29
54	On the Correlation Between Thermal Cycle and Formation of Intermetallic Phases at the Interface of Laserâ€Welded Aluminumâ€ S teel Overlap Joints. Advanced Engineering Materials, 2012, 14, 464-472.	1.6	27

#	Article	IF	CITATIONS
55	Laser metal deposition of refractory high-entropy alloys for high-throughput synthesis and structure-property characterization. International Journal of Extreme Manufacturing, 2021, 3, 015201.	6.3	27
56	Spinodal decomposition versus classical γ′ nucleation in a nickel-base superalloy powder: An in-situ neutron diffraction and atomic-scale analysis. Acta Materialia, 2020, 200, 959-970.	3.8	25
57	Purified oxygen- and nitrogen-modified multi-walled carbon nanotubes as metal-free catalysts for selective olefin hydrogenation. Journal of Energy Chemistry, 2013, 22, 312-320.	7.1	24
58	Sequential Growth of Zinc Oxide Nanorod Arrays at Room Temperature via a Corrosion Process: Application in Visible Light Photocatalysis. ACS Applied Materials & Interfaces, 2014, 6, 18728-18734.	4.0	24
59	Size and size distribution of apatite crystals in sauropod fossil bones. Palaeogeography, Palaeoclimatology, Palaeoecology, 2011, 310, 108-116.	1.0	22
60	PEALD of HfO ₂ Thin Films: Precursor Tuning and a New Near-Ambient-Pressure XPS Approach to in Situ Examination of Thin-Film Surfaces Exposed to Reactive Gases. ACS Applied Materials & Interfaces, 2019, 11, 28407-28422.	4.0	21
61	TEM study of the interface in ceramic-reinforced aluminum-based composites. Materials Chemistry and Physics, 2003, 81, 323-325.	2.0	20
62	Interface engineering and characterization at the atomic-scale of pure and mixed ion layer gas reaction buffer layers in chalcopyrite thin-film solar cells. Progress in Photovoltaics: Research and Applications, 2015, 23, 705-716.	4.4	20
63	Transmission Electron Microscopy of a CMSX-4 Ni-Base Superalloy Produced by Selective Electron Beam Melting. Metals, 2016, 6, 258.	1.0	20
64	Indentation size effects in spherical nanoindentation analyzed by experiment and non-local crystal plasticity. Materialia, 2018, 3, 21-30.	1.3	19
65	Direct monophasic replacement of fatty acid by DMSA on SPION surface. Applied Surface Science, 2012, 258, 9685-9691.	3.1	18
66	CNT-TiO2â^î^´Composites for Improved Co-Catalyst Dispersion and Stabilized Photocatalytic Hydrogen Production. Catalysts, 2015, 5, 270-285.	1.6	18
67	Segregation Phenomena in Size-Selected Bimetallic CuNi Nanoparticle Catalysts. Journal of Physical Chemistry B, 2018, 122, 919-926.	1.2	18
68	Quantitative analysis of grain boundary diffusion, segregation and precipitation at a sub-nanometer scale. Acta Materialia, 2022, 225, 117522.	3.8	18
69	Correlation of Microstructure and Properties of Cold Gas Sprayed INCONEL 718 Coatings. Journal of Thermal Spray Technology, 2020, 29, 1455-1465.	1.6	17
70	Direct liquid injection chemical vapor deposition of ZrO2 films from a heteroleptic Zr precursor: interplay between film characteristics and corrosion protection of stainless steel. Journal of Materials Research and Technology, 2021, 13, 1599-1614.	2.6	16
71	Palladium Nanoparticles Supported on Nitrogenâ€Doped Carbon Nanotubes as a Releaseâ€andâ€Catch Catalytic System in Aerobic Liquidâ€Phase Ethanol Oxidation. ChemCatChem, 2016, 8, 1269-1273.	1.8	14
72	Correlative chemical and structural investigations of accelerated phase evolution in a nanocrystalline high entropy alloy. Scripta Materialia, 2020, 183, 122-126.	2.6	14

#	Article	IF	CITATIONS
73	Synthesis of titanium carbonitride coating layers with star-shaped crystallite morphology. Materials Letters, 2012, 68, 71-74.	1.3	13
74	Short Communication on "Coarsening of Y-rich oxide particles in 9%Cr-ODS Eurofer steel annealed at 1350Ã, Ã,°C― Journal of Nuclear Materials, 2017, 484, 283-287.	1.3	13
75	Effect of off-stoichiometric compositions on microstructures and phase transformation behavior in Ni-Cu-Pd-Ti-Zr-Hf high entropy shape memory alloys. Journal of Alloys and Compounds, 2021, 857, 157467.	2.8	13
76	A new metalorganic chemical vapor deposition process for MoS ₂ with a 1,4-diazabutadienyl stabilized molybdenum precursor and elemental sulfur. Dalton Transactions, 2020, 49, 13462-13474.	1.6	12
77	Microstructure and mechanical properties in the thin film system Cu-Zr. Thin Solid Films, 2018, 645, 193-202.	0.8	10
78	High-throughput characterization of Ag–V–O nanostructured thin-film materials libraries for photoelectrochemical solar water splitting. International Journal of Hydrogen Energy, 2020, 45, 12037-12047.	3.8	10
79	Validation of a Terminally Amino Functionalized Tetraâ€Alkyl Sn(IV) Precursor in Metal–Organic Chemical Vapor Deposition of SnO 2 Thin Films: Study of Film Growth Characteristics, Optical, and Electrical Properties. Advanced Materials Interfaces, 2019, 6, 1801540.	1.9	9
80	Phase decomposition in a nanocrystalline CrCoNi alloy. Scripta Materialia, 2020, 188, 259-263.	2.6	9
81	Sensing and electrocatalytic activity of tungsten disulphide thin films fabricated <i>via</i> metal–organic chemical vapour deposition. Journal of Materials Chemistry C, 2021, 9, 10254-10265.	2.7	8
82	Crystallographic Orientation Analysis of Nanocrystalline Tungsten Thin Film Using TEM Precession Electron Diffraction and SEM Transmission Kikuchi Diffraction. Microscopy and Microanalysis, 2021, 27, 237-249.	0.2	7
83	The software tool for lattice parameters determination from nanoareas using CBED patterns. Materials Chemistry and Physics, 2003, 81, 233-236.	2.0	6
84	High-temperature dislocation plasticity in the single-crystal superalloy LEK94. Journal of Microscopy, 2006, 223, 295-297.	0.8	6
85	Laser metal deposition of Al0.6CoCrFeNi with Ti & C additions using elemental powder blends. Surface and Coatings Technology, 2021, 418, 127233.	2.2	6
86	Structure Zone Investigation of Multiple Principle Element Alloy Thin Films as Optimization for Nanoindentation Measurements. Materials, 2020, 13, 2113.	1.3	5
87	Effect of Grain Statistics on Micromechanical Modeling: The Example of Additively Manufactured Materials Examined by Electron Backscatter Diffraction. Advanced Engineering Materials, 2020, 22, 1901416.	1.6	5
88	Influence of low Bi contents on phase transformation properties of VO ₂ studied in a VO ₂ :Bi thin film library. RSC Advances, 2021, 11, 7231-7237.	1.7	5
89	Influence of Mo/Cr ratio on the lamellar microstructure and mechanical properties of as-cast Al0.75CoCrFeNi compositionally complex alloys. Journal of Alloys and Compounds, 2022, 899, 163183.	2.8	5
90	Dislocation engineering and its effect on the oxidation behaviour. Materials at High Temperatures, 2012, 29, 116-122.	0.5	4

#	Article	IF	CITATIONS
91	TEM replica analysis of particle phases in a tempered martensite ferritic Cr steel after long term creep. Materials Characterization, 2021, 181, 111396.	1.9	4
92	Enhanced Quantum Confined Stark Effect in a mesoporous hybrid multifunctional system. Solid State Communications, 2014, 187, 48-52.	0.9	2
93	Data regarding the influence of Al, Ti, and C additions to as-cast Al0.6CoCrFeNi compositionally complex alloys on microstructures and mechanical properties. Data in Brief, 2019, 27, 104742.	0.5	1
94	Microstructure Characterization of Tool Steel Claddings Coâ€Extruded on Low Alloyed Steel Substrates. Advanced Engineering Materials, 2009, 11, 364-369.	1.6	0